Journal of Applied Fluid Mechanics , Vol. 9, No. 1, pp. 463-474, 2016.
Available online at www.jafmonline.net, ISSN 1735-3572, EISSN 1735-3645.
DOI: 10.18869/acadpub.jafm.68.224.23666

Forced Convective Flow of a Nanoliquid due to a Stretching Cylinder with Free Stream

D. Sinha[1†] , P. Jain[2], P. G. Siddheshwar[3] and N. S. Tomer[4]

[1] *Department of Mathematics, South Asian University, Akbar Bhawan, Chanakyapuri, New Delhi 110 021, India*
[2] *Department of Mathematics & Statistics, Banasthali University, Banasthali 304 022, Rajasthan, India*
[3] *Department of Mathematics, Central College Campus, Bangalore University, Bangalore 560 001, India*
[4] *Department of Mathematics, F.G.M. Govt. College, Adampur (Hisar), Haryana, India.*

† *Corresponding Author Email*: *deepasinha2001@gmail.com*

(Received June 27, 2014; accepted December 10, 2014)

ABSTRACT

Steady, transverse boundary layer flow and heat transfer caused by an exponentially stretching cylinder of constant radius immersed in an uniform flow of an incompressible, viscous nanoliquid are considered in the present study. The paper discusses a systematic procedure of obtaining a local similarity transformation that reduces the governing partial differential equations into ordinary differential equations. Power series solution is then obtained for velocity, temperature and nanoparticle concentration distributions using the uni-variate differential transform method. Help is sought from Domb-Sykes plots in making a decision on the minimum number of terms required in the power series expansion to ensure convergence. Radius of convergence is quite naturally suggested by these plots. Padé approximants are then appropriately decided upon to increase the radius of convergence. The algorithm used succeeds in capturing boundary effects, free stream flow effects and nanoparticle effects on flow and heat transfer. An important finding of the paper is the prediction of accelerated cooling of the stretching cylinder due to the nanoparticles in the cooling liquid. In having a desirable property for the extruding cylinder nanoliquid coolant seems an attractive proposition.

Keywords: Nanoliquid; Stretching cylinder; Free stream; Domb-Sykes; Buongiorno.

NOMENCLATURE

C_p	specific heat at constant pressure	γ	transverse curvature
C_f	skin friction coefficient	η	similarity variable
p	dimensionless pressure	κ	thermal conductivity
R	radius of the cylinder	λ	free stream parameter
Re_x	local Reynolds number	μ	dynamic viscosity
$\bar{u}_w(\bar{x})$	stretching velocity in axial direction	ϑ	kinematic viscosity
$\bar{u}_\infty(\bar{x})$	free stream velocity in axial direction	θ	dimensionless temperature
u, v	dimensionless axial and radial velocity components	ρ	density
v_w	dimensionless suction/injection velocity	τ_w	surface shear stress
x, r	dimensionless axial and radial coordinates	ψ	stream function

1. INTRODUCTION

The boundary layer flow and heat transfer on continuous moving sheet or cylinder are of practical importance in a number of engineering processes like continuous casting and spinning of fibers, polymer fiber coating in fiber technology, aerodynamic extrusion of plastic sheets, cooling of an infinite metallic plate in a cooling bath, the boundary layer along a liquid film in condensation process, coating of cylindrical wires, a polymer sheet or filament extruded continuously from a die, or a long tread traveling between a feed roll and a wind-up roll. In view of these applications, boundary layer flow behavior over a continuous solid surface moving with constant speed in a Newtonian fluid was initially studied by Sakiadis (1961a, 1961b). Crane (1970, 1975) extended the work for flow of a viscous fluid past a linearly stretching surface and the axisymmetric flow due

to a stretching cylinder. Lin and Shih (1980) considered the laminar boundary layer and heat transfer along horizontally and vertically moving cylinders with constant velocity and found that the similarity solutions could not be obtained due to the curvature effect of the cylinder. The steady flow of viscous and incompressible fluid outside of a stretching hollow cylinder in an ambient fluid at rest has been studied by Wang (1988, 2002, 2007, 2009, 2012) and Wang and Ng (2011). There are several works covering the effect of transverse curvature on forced, free and mixed convective flows over a cylinder (Ishak et al. (2008), Ishak and Nazar (2009), Bachok and Ishak (2009, 2010), Rangi and Ahmed (2012)). In some works the flow over cylinders is considered to be two-dimensional when the body radius is very large compared to the boundary layer thickness. For a slender cylinder, the radius of the cylinder is of the same order as the boundary layer thickness and hence the flow is axisymmetric. In this case, the governing equations contain the transverse curvature term in the momentum and temperature equations.

Several researchers considered various aspects of momentum, heat and mass transfer characteristics in boundary layer flow over a exponentially stretching surface (Elbashbeshy (2001), Khan and Sanjayanand (2005), Sanjayanand and Khan (2006), Sajid and Hayat (2008), Bidin and Nazar (2009), Siddheshwar et al. (2014a, 2014b)). Gupta and Mahapatra (2003), Sharma and Singh (2009), Singh et al. (2012) analyzed stagnation point flow towards a stretching surface and reported that a boundary layer is formed when stretching velocity is less than the free stream velocity. As the stretching velocity exceeds the free stream velocity then an inverted boundary layer is formed. Sparse literature is available on stretching sheet problems, stretching exponentially, in a fluid that is flowing with uniform velocity called generally as uniform free stream (Vajravelu and Hadjinicolaou (1997), Magyari and Keller (1999), Abo-Eldahab and Ghonaim (2003), Partha et al. (2005), Gireesha et al. (2014) and Xu (2005)).

In the context of the cooling application situations mentioned above it seems desirable to consider high thermal conductivity liquids. Nanoliquids (Choi and Eastman (1995)) have been shown to possess high thermal conductivity and hence exhibit convective heat transfer performance. This aspect can prove useful in having a desirable final product in application situations discussed earlier. Recently, the study of convective transport of nanoliquids has gained considerable importance due to such applications. Numerous investigations on the stretching sheet have been made considering nanoliquid (Yacob et al. (2011), Hamad (2011), Noghrehabadi et al. (2011), Nourazar et al. (2011), Vajravelu et al. (2011), Rosmila et al. (2012), Khan and Pop (2010), Makinde and Aziz (2011), Rana and Bhargava (2012), VanGorder et al. (2010), Hassani et al. (2011), Noghrehabadi et al. (2012), Anwar et al. (2012), Gashemi and Aminossadati (2009), Devi and Andrews (2011), Hamad et al. (2011), Kousar and Liao (2011), Akyildiz et al. (2011), Vajravelu et al. (2013), Sheikhzadeh et al. (2011) and references therein).

From the literature survey it is obvious that there is no reported work on the exponentially stretching cylinder problem involving a nanoliquid taking free stream into account. In the present paper, we find the velocity and temperature fields for boundary layer flow of a nanoliquid past a stretching cylinder using the DTM-Domb Sykes-Padé technique. We study the influence of free stream, curvature, suction/injection, Prandtl number, Brownian diffusion and thermophoresis on velocity and temperature fields, skin-friction coefficient and Nusselt number.

2. MATHEMATICAL FORMULATION

A steady, two-dimensional, boundary layer flow of an incompressible nanoliquid over an exponentially stretching cylinder of constant radius is considered. In the laminar sublayer near the wall, Brownian diffusion and thermophoresis are important for nanoparticles of any material and size (Buongiorno (2006)). Based on this hypothesis the physical model and coordinate system considered are as shown in Figure 1. The steady governing equations conservation of mass, momentum, thermal energy and nanoparticles including the dynamic effects of nanoparticles (eqs. 14, 17, 18 and 23 in Buongiorno (2006)) using the boundary layer approximations can be written as follows:

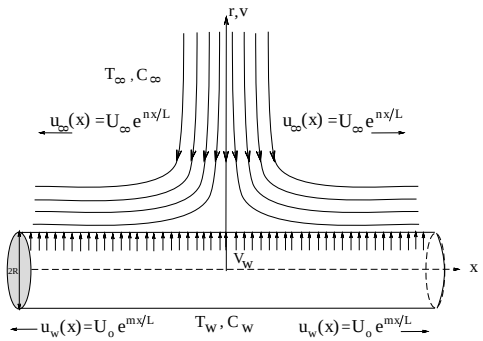

Fig. 1. Schematic diagram of the problem

$$\frac{\partial \bar{u}}{\partial \bar{x}} + \frac{\partial \bar{v}}{\partial \bar{r}} + \frac{1}{\bar{r}}\bar{v} = 0, \tag{1}$$

$$\bar{u}\frac{\partial \bar{u}}{\partial \bar{x}} + \bar{v}\frac{\partial \bar{u}}{\partial \bar{r}} = -\frac{1}{\rho}\frac{\partial \bar{p}}{\partial \bar{x}} + \vartheta\left(\frac{\partial^2 \bar{u}}{\partial \bar{r}^2} + \frac{1}{\bar{r}}\frac{\partial \bar{u}}{\partial \bar{r}}\right), \tag{2}$$

$$\bar{u}\frac{\partial \bar{T}}{\partial \bar{x}}+\bar{v}\frac{\partial \bar{T}}{\partial \bar{r}}=\alpha\left(\frac{\partial^2 \bar{T}}{\partial \bar{r}^2}+\frac{1}{\bar{r}}\frac{\partial \bar{T}}{\partial \bar{r}}\right)+\tau\left\{D_B\left(\frac{\partial \bar{c}}{\partial \bar{r}}\frac{\partial \bar{T}}{\partial \bar{r}}\right)+\frac{D_T}{T_\infty}\left(\frac{\partial \bar{T}}{\partial \bar{r}}\right)^2\right\}, \quad (3)$$

$$\bar{u}\frac{\partial \bar{C}}{\partial \bar{x}}+\bar{v}\frac{\partial \bar{C}}{\partial \bar{r}}=D_B\left(\frac{\partial^2 \bar{C}}{\partial \bar{r}^2}+\frac{1}{\bar{r}}\frac{\partial \bar{C}}{\partial \bar{r}}\right)+\frac{D_T}{T_\infty}\left(\frac{\partial^2 \bar{T}}{\partial \bar{r}^2}+\frac{1}{\bar{r}}\frac{\partial \bar{T}}{\partial \bar{r}}\right). \quad (4)$$

where $\bar{u}$ and $\bar{v}$ are the velocity components in the axial and radial directions $\bar{x}$ and $\bar{r}$ respectively, $\bar{T}$ and T_∞ are the local temperature and the constant temperature far away from sheet of the nanoliquid, $\bar{C}$ is the volume fraction of solid nanoparticles. $\bar{p}$, ρ, ϑ, $\alpha=\kappa/(\rho C_p)$ and κ are pressure, density, kinematic viscosity, thermal diffusivity and thermal conductivity of the fluid respectively, $\tau=(\rho C_p)_p/(\rho C_p)_{bf}$ is the ratio of heat capacities of solid particles and base fluid, D_B and D_T are the Brownian and thermophoretic diffusion coefficients. The boundary conditions are taken to be

$$\bar{r}=R:\bar{u}=\bar{u}_w(\bar{x})=U_0 e^{m\frac{\bar{x}}{L}},\bar{v}=\bar{v}_w,\bar{T}=T_w,\bar{C}=C_w,$$
$$\bar{r}\to\infty:\bar{u}=\bar{u}_\infty(\bar{x})=U_\infty e^{n\frac{\bar{x}}{L}},\bar{T}=T_\infty,\bar{C}=C_\infty, \quad (5)$$

where U_0, U_∞, L, T_w, C_w and C_∞ are characteristic stretching velocity, characteristic free stream velocity, characteristic length, surface temperature, nanoparticle concentration at the surface and in the quiescent fluid respectively, $\bar{v}_w$ is suction/injection velocity when $\bar{v}_w<0$ and $\bar{v}_w>0$ respectively. m and n are the stretching exponents taken in general.

3. METHOD OF SOLUTION

Introducing the following non-dimensional variables

$$x=\frac{\bar{x}}{L},\ r=\frac{\bar{r}}{R},\ u=\frac{\bar{u}}{U_0},\ v=\frac{\bar{v}L}{U_0R},\ v_w=\frac{\bar{v}_wL}{U_0R},\ p=\frac{\bar{p}}{\rho U_0^2},\ T=\frac{\bar{T}-T_\infty}{T_w-T_\infty},\ C=\frac{\bar{C}-C_\infty}{C_w-C_\infty}, \quad (6)$$

eqs. (1-4) can be written in non-dimensional form as:

$$\frac{\partial u}{\partial x}+\frac{\partial v}{\partial r}+\frac{1}{r}v=0, \quad (7)$$

$$u\frac{\partial u}{\partial x}+v\frac{\partial u}{\partial r}=-\frac{dp}{dx}+\gamma^2\left(\frac{\partial^2 u}{\partial r^2}+\frac{1}{r}\frac{\partial u}{\partial r}\right), \quad (8)$$

$$u\frac{\partial T}{\partial x}+v\frac{\partial T}{\partial r}=\frac{\gamma^2}{Pr}\left(\frac{\partial^2 T}{\partial r^2}+\frac{1}{r}\frac{\partial T}{\partial r}\right)+\gamma^2\left[Nb\left(\frac{\partial C}{\partial r}\frac{\partial T}{\partial r}\right)+Nt\left(\frac{\partial T}{\partial r}\right)^2\right], \quad (9)$$

$$u\frac{\partial C}{\partial x}+v\frac{\partial C}{\partial r}=\frac{\gamma^2}{Le}\left[\left(\frac{\partial^2 C}{\partial r^2}+\frac{1}{r}\frac{\partial C}{\partial r}\right)+\frac{Nt}{Nb}\left(\frac{\partial^2 T}{\partial r^2}+\frac{1}{r}\frac{\partial T}{\partial r}\right)\right], \quad (10)$$

where $\gamma=\sqrt{\vartheta L/R^2U_0}$, $Pr=\vartheta/\alpha$, $Nb=\tau D_B(C_w-C_\infty)/\vartheta$, $Nt=\tau D_T(T_w-T_\infty)/\vartheta T_\infty$ and $Le=\vartheta/D_B$ are transverse curvature parameter, Prandtl number, Brownian motion parameter, thermophoresis parameter and Lewis number. The boundary conditions (5) in non-dimensional form are:

$$r=1\ :\ u=e^{mx},\ v=v_w,\ T=1,\ C=1,$$
$$r\to\infty:\ u=\lambda e^{nx},\ T=0,\ C=0, \quad (11)$$

where $\lambda=U_\infty/U_0$ is called free stream parameter. In free stream $u=u_\infty=\lambda e^{nx}$ reduces eq. (8) to

$$u_\infty\frac{du_\infty}{dx}=-\frac{dp}{dx}, \quad (12)$$

which gives,

$$\frac{dp}{dx}=-\lambda^2 n e^{2nx}, \quad (13)$$

eliminating $\frac{dp}{dx}$ from eq. (8) using eq. (13), we get

$$u\frac{\partial u}{\partial x}+v\frac{\partial u}{\partial r}=\gamma^2\left(\frac{\partial^2 u}{\partial r^2}+\frac{1}{r}\frac{\partial u}{\partial r}\right)+\lambda^2 n e^{2nx}. \quad (14)$$

3.1 Procedure of obtaining local similarity transformation

To attain the similarity solution of eqs. (7), (9), (10) and (14) with (11), we introduce the stream function $\psi(x,r)$ with velocity components $u=\frac{1}{r}\frac{\partial\psi}{\partial r}$ and $v=-\frac{1}{r}\frac{\partial\psi}{\partial x}$,

$$\frac{\partial\psi}{\partial r}\frac{\partial^2\psi}{\partial x\partial r}+\frac{1}{r}\frac{\partial\psi}{\partial x}\frac{\partial\psi}{\partial r}-\frac{\partial\psi}{\partial x}\frac{\partial^2\psi}{\partial r^2}=\lambda^2 n e^{2nx}r^2+\gamma^2\left(r\frac{\partial^3\psi}{\partial r^3}-\frac{\partial^2\psi}{\partial r^2}+\frac{1}{r}\frac{\partial\psi}{\partial r}\right), \quad (15)$$

$$\frac{\partial\psi}{\partial r}\frac{\partial T}{\partial x}-\frac{\partial\psi}{\partial x}\frac{\partial T}{\partial r}=r\gamma^2\left[\frac{1}{Pr}\left(\frac{\partial^2 T}{\partial r^2}+\frac{1}{r}\frac{\partial T}{\partial r}\right)+Nb\left(\frac{\partial C}{\partial r}\frac{\partial T}{\partial r}\right)+Nt\left(\frac{\partial T}{\partial r}\right)^2\right], \quad (16)$$

$$\frac{\partial\psi}{\partial r}\frac{\partial C}{\partial x}-\frac{\partial\psi}{\partial x}\frac{\partial C}{\partial r}=\frac{\gamma^2}{Le}\left[\left(r\frac{\partial^2 C}{\partial r^2}+\frac{\partial C}{\partial r}\right)+\frac{Nt}{Nb}\left(r\frac{\partial^2 T}{\partial r^2}+\frac{\partial T}{\partial r}\right)\right], \quad (17)$$

$$r=1 \;:\; \frac{\partial \psi}{\partial r} = re^{mx},\ \frac{\partial \psi}{\partial x} = -rv_w,\ T=1,\ C=1,$$
$$r\to\infty \;:\; \frac{\partial \psi}{\partial r} = r\lambda e^{nx},\ T=0,\ C=0. \qquad (18)$$

The following transformation will now be used in eq. (15)-(18)

$$\psi(x,\eta) = Af(\eta)e^{sx},\ T=\theta(\eta),\ C=\phi(\eta),$$
$$\eta = B(r^2-1)e^{tx}, \qquad (19)$$

where A, B, s, t are to be determined. The transformations given by eq. (19) has been obtained by using Lie-group transformation method. Using the transformation in eqs. (15)-(18), we get the following BVP

$$2\gamma^2\left\{\left(\eta+Be^{tx}\right)f'''+f''\right\}+Ase^{sx}ff''$$
$$-A(s+t)e^{sx}f'^2+\frac{\lambda^2 ne^{(2n-s-2t)x}}{4AB^2}=0, \qquad (20)$$

$$2\gamma^2\left\{\left(\eta+Be^{tx}\right)\theta''+\theta'\right\}+Pr\left[Ase^{sx}f\theta'\right.$$
$$\left.+2\gamma^2\left(\eta+Be^{tx}\right)\left(Nb\theta'\phi'+Nt\theta'^2\right)\right]=0, \qquad (21)$$

$$2\gamma^2\left\{\left(\eta+Be^{tx}\right)\phi''+\phi'\right\}+LeAse^{sx}f\phi'$$
$$+2\gamma^2\frac{Nt}{Nb}\left\{\left(\eta+Be^{tx}\right)\theta''+\theta'\right\}=0, \qquad (22)$$

$$f(0)=\frac{-v_w}{Ase^{sx}}, f'(0)=\frac{e^{(m-s-t)x}}{2AB}, \theta(0)=1, \phi(0)=1,$$
$$f'(\infty)=\frac{\lambda e^{(n-s-t)x}}{2AB}, \theta(\infty)=0, \phi(\infty)=0, \qquad (23)$$

The equations dictate the choice $A=\sqrt{2}\gamma$, $B=\frac{1}{2\sqrt{2}\gamma}$, $m=n=1$ and $s=t=\frac{1}{2}$. With this choice, the local similarity variable take the following form

$$\psi=\sqrt{2}e^{\frac{x}{2}}\gamma f(\eta), T=\theta(\eta), C=\phi(\eta),$$
$$\eta=\left(\frac{r^2-1}{2\sqrt{2}\gamma}\right)e^{\frac{x}{2}}. \qquad (24)$$

The above transformations leads to boundary value problems:

$$(1+2\eta\gamma_x)f'''+2\gamma_x f''+ff''-2f'^2+2\lambda^2=0, \qquad (25)$$

$$(1+2\eta\gamma_x)\theta''+2\gamma_x\theta'+Pr\left[f\theta'\right.$$
$$\left.+(1+2\eta\gamma_x)\left(Nb\theta'\phi'+Nt\theta'^2\right)\right]=0, \qquad (26)$$

$$(1+2\eta\gamma_x)\phi''+2\gamma_x\phi'+Lef\phi'$$
$$+\frac{Nt}{Nb}\left[2\gamma_x\theta'+(1+2\eta\gamma_x)\theta''\right]=0, \qquad (27)$$

$$f(0)=-V_{wx}, f'(0)=1, \theta(0)=1, \phi(0)=1,$$
$$f'(\infty)=\lambda, \theta(\infty)=0, \phi(\infty)=0, \qquad (28)$$

where prime denotes differentiation with respect to η, $\gamma_x=\sqrt{2}\gamma e^{-x/2}$ is the local transverse curvature parameter and $V_{wx}=v_w\sqrt{2}e^{-x/2}$ is local suction/injection parameter.

3.2 Algorithm

The system of non-linear differential eqs. (25)-(27) subject to the boundary conditions (28), constitute a two-point boundary value problem. The solution of this system in the form of a rational approximation of the power series in η is obtained in this paper by following the algorithm below:

1. Convert the boundary value problem to an equivalent initial value problem (EIVP) as done by Abel et al. (2011). The decision on ∞ is made computationally. ∞ is so chosen that the boundary condition of eq. (23) is satisfied. In our problem ∞ turns out to be around 6. The initial conditions of the EIVP now are:

$$\left.\begin{array}{l} f(0)=-V_{wx}, f'(0)=1, f''(0)=-A_1, \\ \theta(0)=1, \theta'(0)=-A_2, \\ \phi(0)=1, \phi'(0)=-A_3. \end{array}\right\} \qquad (29)$$

   where A_1, A_2 and A_3 are obtained by shooting technique as functions of the parameters λ, Pr, γ, Nb, Nt, Le and V_{wx} of the problem.

2. Obtain the power series solution of the EIVP by using the uni-variate differential transform method (DTM) of Zhou (1986). The differential transform on the initial conditions (29) and on the system of nonlinear differential equations (25)-(27), the $F[k]$'s, $\Theta[k]$'s and $\Phi[k]$'s

gives us (Sinha et al. (2014)),

$$
\begin{aligned}
&F[0] = -V_{wx}, F[1] = 1, F[2] = -\tfrac{A_1}{2},\\
&\Theta[0] = 1, \Theta[1] = -A_2,\\
&\Phi[0] = 1, \Phi[0] = -A_3,\\
&F[k+1]\\
&= \tfrac{-1}{k(k^2-1)}\left[2\gamma_x k(k-1)^2 F[k] + 2\lambda^2 \delta[k-2]\right.\\
&+ \sum_{r=0}^{k-2}(k-r-1)\{(k-r)F[r]F[k-r]\\
&\left. -2(r+1)F[r+1]F[k-r-1]\}\right],\\
&\Theta[k+1] = \tfrac{-1}{k(k+1)}\left[2\gamma_x k^2 \Theta[k]\right.\\
&+ Pr\sum_{r=0}^{k-1} F[r](k-r)\Theta[k-r]\\
&+ Prk\Theta[k]\,(Nb\Phi[1] + Nt\Theta[1])\\
&+ Pr(1+2\gamma_x)\sum_{r=0}^{k-2}\{(r+1)(k-r-1)\Theta[r+1]\\
&\left.(Nb\Phi[k-r-1] + Nt\Theta[k-r-1])\}\right],\\
&\Phi[k+1] = \tfrac{-1}{k(k+1)}\left[2\gamma_x k^2 \Phi[k]\right.\\
&+ Le\sum_{r=0}^{k-1} F[r](k-r)\Phi[k-r]\\
&\left. + \tfrac{Nt}{Nb}\left\{2\gamma_x k^2\Theta[k] + k(k+1)\Theta[k+1]\right\}\right].
\end{aligned}
\tag{30}
$$

The inverse differential transform now yields the power series solution for $f(\eta)$, $\theta(\eta)$ and $\phi(\eta)$ in the form (Sinha et al. (2014)):

$$f(\eta) = \sum_{k=0}^{N} F[k]\eta^k, \tag{31}$$

$$\theta(\eta) = \sum_{k=0}^{N} \Theta[k]\eta^k, \tag{32}$$

$$\phi(\eta) = \sum_{k=0}^{N} \Phi[k]\eta^k. \tag{33}$$

3. The decision on the minimum number of terms required in the power series solution obtained by DTM is made after inverse Domb-Sykes plots (Domb and Sykes (1957), Mercer and Roberts (1990)) shown in figures 2(a) and 2(b). The minimum number of terms required in the power series for $f(\eta)$, $\theta(\eta)$ and $\phi(\eta)$ are 15, 20 and 20 respectively. Details of this procedure are given in the work of VanDyke (1974).

4. Use the correct Padé-approximant $[m,n]$ for a given N to improve the convergence of the power series solution. Padé-approximant is nothing but a rational approximation that gives convergent solution when $m < n$. The rational approximation is a ratio of two finite degree polynomials (Baker (1975)).

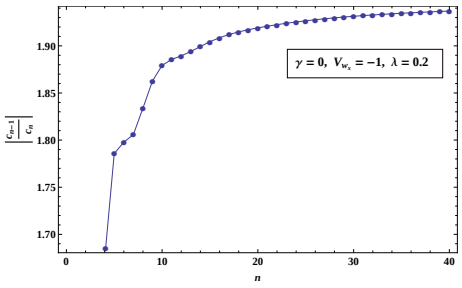

(a) $f(\eta)$

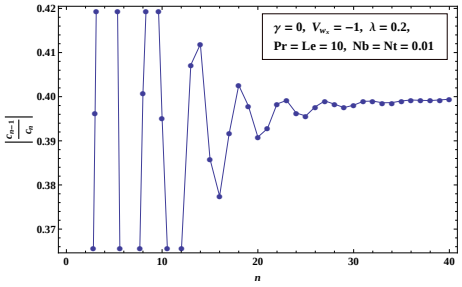

(b) $\theta(\eta)$

Fig. 2. Sample inverse Domb-Sykes plots for (a) $f(\eta)$ and (b) $\theta(\eta)$.

5. Increase N and follow steps 2 and 3 till desired accuracy is obtained. The satisfaction of the conditions at ∞ by the rational approximation serves as an indicator for the validation of the obtained solution.

4. Results and Discussion

The focus of the present study is on bringing out the effects of the free stream parameter, the transverse curvature parameter and the suction/injection parameter along with Prandtl number, Brownian motion and thermophoresis parameters, Lewis number on the velocity profile, skin friction, wall temperature or wall temperature gradient and the nanoparticle volume fraction. To validate the results, comparison of the skin friction coefficient, the wall temperature gradient and the wall temperature with those of previously published works in limiting cases is reported. When the radius of cylinder $R \to \infty$, the transverse curvature parameter $\gamma \to 0$ and hence the problem reduces to the stretching sheet case as shown in Figure 3 in the absence of transverse curvature. In Table 1 and 2 the results of present study are compared with the results of Elbashbeshy (2001) for the reduced skin-friction coefficient $-f''(0)$ and for the reduced Nusselt number $-\theta'(0)$ at different values of suction parameter V_{wx} in absence of free stream ($\lambda = 0$) for boundary layer flow of Newtonian liquid (when $Nb = Nt = 0$) over an exponentially stretching sheet ($\gamma = 0$).

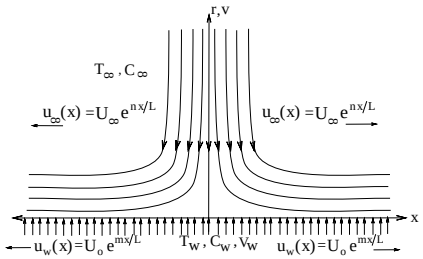

Fig. 3. Limiting Case: Exponentially Stretching Sheet

4.1 Dimensionless Physical Quantities

4.11 Local Skin Friction Coefficient

$$C_{fx} = \frac{\tau_w}{\rho u_w^2} = \frac{-\mu\left(\frac{\partial u^*}{\partial r^*}\right)_{r^*=R}}{\rho u_w^2} = -Re_x^{-1/2} f''(0).$$

$$\Rightarrow C_{fxr} = Re_x^{1/2} C_{fx} = A_1. \tag{34}$$

4.12 Local Nusselt Number

$$Nu_x = \frac{x^*\left[-\kappa\frac{\partial T^*}{\partial r^*} - (\rho C_p)_p (T^* - T_\infty)\left\{D_B\frac{\partial C^*}{\partial r^*} + \frac{D_T}{T_\infty}\frac{\partial T^*}{\partial r^*}\right\}\right]_{r^*=R}}{\kappa(T_w - T_\infty)}$$

$$= -Re_x^{1/2}\left[(1+PrNt)\theta'(0) + PrNb\phi'(0)\right].$$

$$\Rightarrow Nu_{xr} = Re_x^{-1/2} Nu_x = (1+PrNt)A_2 + PrNbA_3. \tag{35}$$

4.13 Local Sherwood Number

$$Sh_x = \frac{x^*\left(-D_B\frac{\partial C^*}{\partial r^*} - \frac{D_T}{T_\infty}\frac{\partial T^*}{\partial r^*}\right)_{r^*=R}}{D_B(C_w - C_\infty)}$$

$$= Re_x^{1/2}\left[-\phi'(0) - \frac{Nt}{Nb}\theta'(0)\right].$$

$$\Rightarrow Sh_{xr} = Re_x^{-1/2} Sh_x = A_3 + \frac{Nt}{Nb}A_2. \tag{36}$$

The local Reynolds number is given by $Re_x = \frac{u_w x}{\vartheta}$.

4.2 Velocity Profiles

Figure 4 scrutinizes the variation of velocity profiles with various parameters, the free stream parameter λ, the transverse curvature parameter γ and the suction/injection parameter V_{wx}. Figure 4(a) depicts the variation in dimensionless axial velocity for different values of λ the ratio of free stream velocity to stretching velocity. It can be perceived that a boundary layer is formed when the free stream velocity exceeds the stretching velocity *i.e.* at $\lambda > 1$ whereas an inverted boundary layer is found at $\lambda < 1$ when stretching velocity exceeds free stream velocity. The boundary layer thickness decreases significantly as λ increases at the points where velocity reaches the boundary condition. Physically, when λ increases, the increase in U_∞ for fixed values of U_0 implies increase in straining motion near the stagnation region resulting in acceleration of free stream which leads to thinning of the boundary layer. Hence surface shear stress also increases. It can be observed that boundary layer does not form for $\lambda = 1$, as the stretching velocity and the free stream velocity are equal.

The effect of surface curvature on the nanoliquid velocity can be observed in fig. 4(b). The nanoliquid velocity decreases very close to the surface in a significant region $0 \le \eta \le 0.3$ with increase in the curvature parameter γ. It happens because the radius of the cylinder reduces on enhancing the curvature and hence the surface area of the cylinder in contact with the nanoliquid reduces. So the shear

Table 1. Comparison of results for the reduced skin-friction coefficient $-f''(0)$ at different values of suction parameter V_{wx} in absence of free stream ($\lambda = 0$) for boundary layer flow of Newtonian liquid (when $Nb = Nt = 0$) over an exponentially stretching sheet ($\gamma = 0$).

V_{wx}	Present results	Elbashbeshy (2001)
0.0	1.282131502	1.28181
−0.2	1.379148613	1.37889
−0.4	1.484572579	1.4839
−0.6	1.598363997	1.59824

Table 2. Comparison of results for the reduced Nusselt number $-\theta'(0)$ at different values of suction parameter V_{wx} and Prandtl number Pr in absence of free stream ($\lambda = 0$) for boundary layer flow of Newtonian liquid (when $Nb = Nt = 0$) over an exponentially stretching sheet ($\gamma = 0$).

V_{wx}	Pr	Present results	Elbashbeshy (2001) (at temperature parameter $\gamma = 0$)
0.0	0.72	0.445683170	0.434717
	1	0.552846579	0.549641
	3	1.121889583	1.122090
	10	2.257320309	2.257430
−0.6	0.72	0.748612591	0.7453955
	1	0.987770427	0.9872843
	3	2.493270352	2.4933760
	10	7.071978100	7.0727307

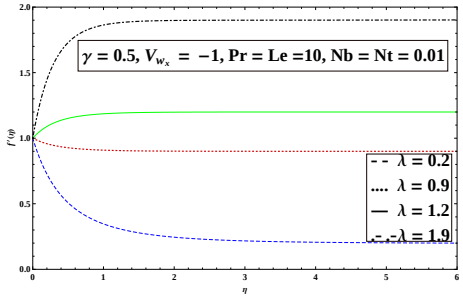

(a) Effect of λ on $f'(\eta)$

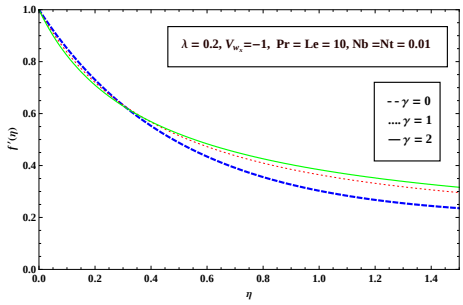

(b) Effect of γ on $f'(\eta)$

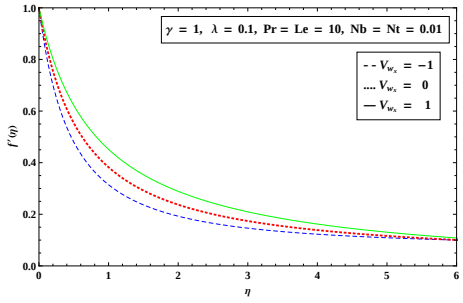

(c) Effect of V_{wx} on $f'(\eta)$

Fig. 4. Variation of velocity profiles with various parameters.

stress per unit area increases due to increases in velocity gradient at the surface. But afterwards velocity starts increasing with γ, as a result the boundary layer thickness also increases. Figure 4(c) describes that an increase in injection velocity ($V_{wx} > 0$) increases the magnitude of axial velocity U, whereas an increase in suction ($V_{wx} < 0$) retards the nanoliquid flow, consequently the momentum boundary thickness decreases with suction.

4.3 Temperature Profiles

Figure 5(a) shows the effect of free stream parameter λ on temperature distribution keeping the other parameters fix. It is found that an increase in λ decreases the temperature at any point in the boundary layer. Temperature profiles in fig. 5(b) show a slight decrease in the temperature of nanoliquid in the neighborhood of the cylinder's surface as γ increases, and afterwards rise, consequently the thermal boundary layer thickness increases. Due to the reduced contact surface area the conduction heat transfer rate also reduces at the surface but after this region temperature increases because of enhanced convection heat transfer in the liquid. Figure 5(c) shows that increasing suction effects suppress temperature. Thermal boundary layer thickness for injection case is significantly greater than for the suction case. It is observed from fig. 5(d) that the temperature profiles decrease rapidly with an increase in the Prandtl number Pr. The temperature effects can be seen very close to the surface as the curves become gradually more steep. This exhibits that at higher Prandtl number, liquid has a thinner thermal boundary layer and this increases the gradient of temperature, hence the reduced Nusselt number also increases. Figure 5(e) presents the effect of the Brownian motion parameter Nb on temperature distribution. The temperature of nanoliquid increases with increase in Nb . As a consequence, the reduced Nusselt number decreases with increase in Nb. Figure 5(f) shows the temperature distribution in the thermal boundary layer for different values of the thermophoresis parameter Nt. As Nt increases, the temperature boundary layer thickness increases and the curves become less steep thereby diminishing the reduced Nusselt number. Figure 5(g) shows the effect of Lewis number Le on the temperature profiles. It is found that the increasing value of Lewis number results in enhancement of the temperature profiles which is noticeable only in a region close to the surface as the curves tend to merge at larger distances from the surface.

4.4 Concentration Profiles

Figure 6(a) illustrates the effect of free stream parameter λ on concentration boundary layer. From the definition of free stream velocity it is obvious that an increase in λ increases the free stream velocity. This is observed in figure 6(a) as a result of this increasing velocity the concentration of nanoparticles in the boundary layer decreases. Figure 6(b) shows that the concentration profiles of nanoliquid increases as the surface curvature increases. Figure 6(c) indicates that suction achieves a strong suppression of nanoparticle species diffusion while injection shows opposite effect on concentration distribution. Figure 6(d) shows that as the Prandtl number Pr increases the concentration boundary layer thickness decreases but the concentration profile increases near the surface as Pr increases. Figure 6(e) shows that the nanoparticle concentration is the decreasing function of Brownian motion parameter Nb. Hence the concentration boundary layer thickness decreases as Nb increases. Figure 6(f) reveals the increasing effect of thermophoresis parameter Nt on the concentration distribution of nanoparticles in nanoliquid and also on reduced Sherwood number. For hot surfaces,

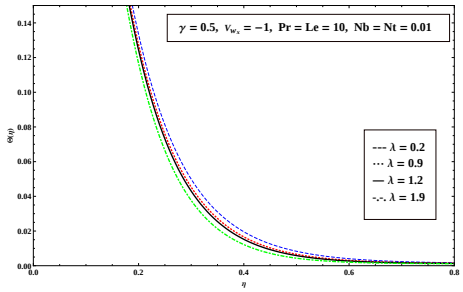

(a) Effect of λ on θ(η)

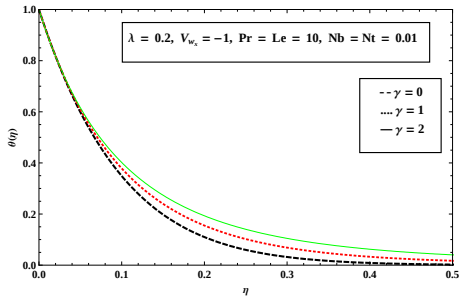

(b) Effect of γ on θ(η)

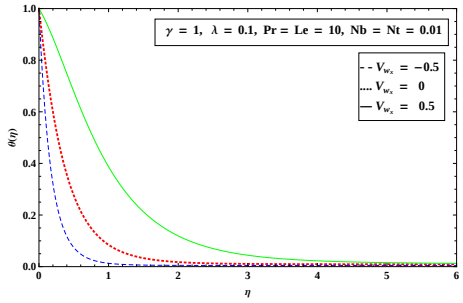

(c) Effect of V_{wx} on θ(η)

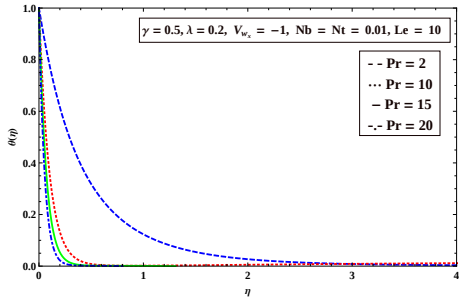

(d) Effect of *Pr* on θ(η)

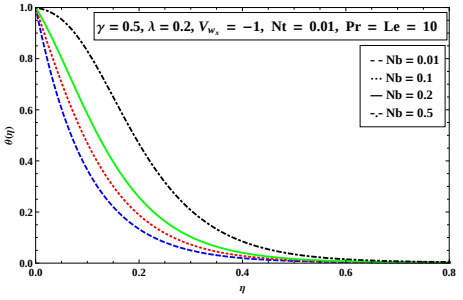

(e) Effect of *Nb* on θ(η)

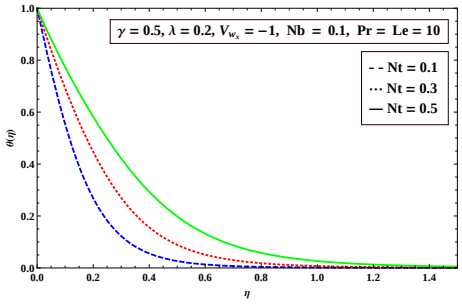

(f) Effect of *Nt* on θ(η)

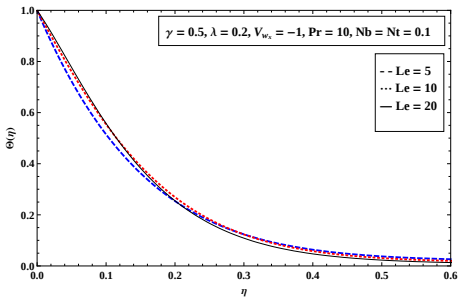

(g) Effect of *Le* on θ(η)

Fig. 5. Variation of temperature profiles with various parameters.

thermophoresis tends to blow the nanoparticle volume fraction boundary layer away from the surface since a hot surface repels the small sized particles from it, thereby forming a relatively particle-free layer near the surface. Figure 6(g) shows the variation of nanoparticle volume fraction for different values of Lewis number *Le*. It can be seen that the concentration of nanoparticles decreases with increase in Lewis number. For a base fluid of certain kinematic viscosity ϑ, a higher Lewis number implies a lower Brownian diffusion coefficient D_B which must result in a shorter penetration depth for the concentration boundary layer.

5. Conclusion

In the present analysis, the steady, two-dimensional boundary layer flow and heat transfer of incompressible, viscous, nanoliquids caused by an exponentially stretching cylinder is discussed. The problem is considered to illustrate the new algorithm DTM-Domb-Sykes-Padé technique. The results are presented for different values of various parameters: free stream parameter, transverse curvature parameter, suction/injection parameter, Prandtl number, Lewis number, Brownian motion and thermophoresis parameters. The greatest advantage of the solution presented in the paper is that the solution is a power series for $f(\eta)$, $\theta(\eta)$ and $\phi(\eta)$ given by equations (31)-(33) in which the coefficients $F[k]$'s, $\Theta[k]$'s and $\Phi[k]$'s are given in equation (30). The combination of DTM, inverse Domb-Sykes plots for $\theta(\eta)$ and $\phi(\eta)$, and Padé approx-

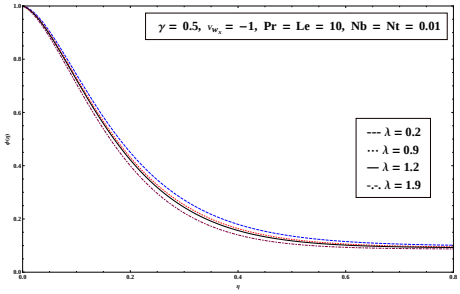

(a) Effect of λ on ϕ(η)

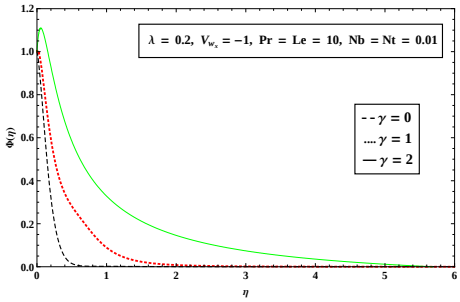

(b) Effect of γ on ϕ(η)

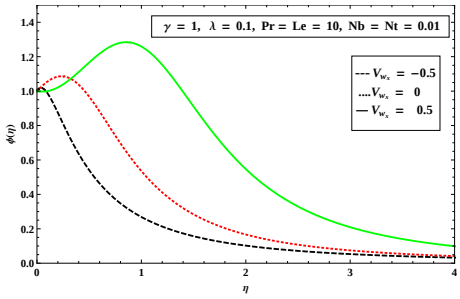

(c) Effect of V_{wx} on ϕ(η)

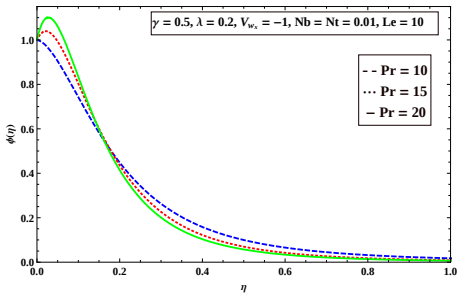

(d) Effect of *Pr* on ϕ(η)

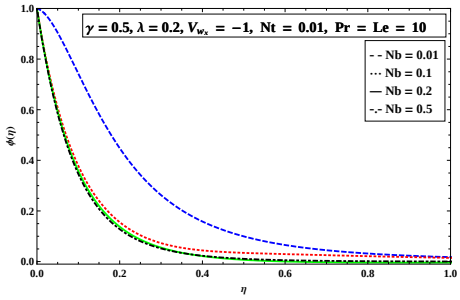

(e) Effect of *Nb* on ϕ(η)

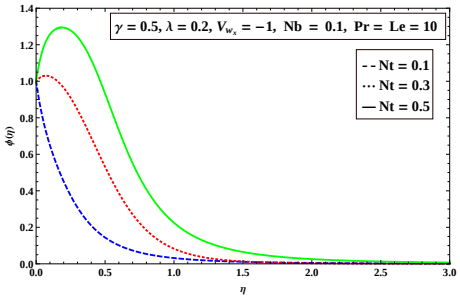

(f) Effect of *Nt* on ϕ(η)

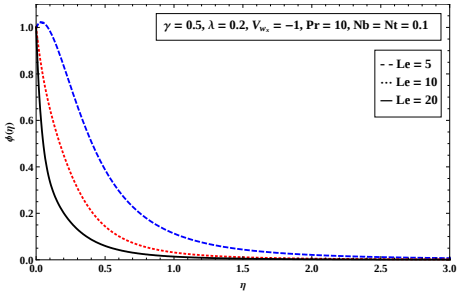

(g) Effect of *Le* on ϕ(η)

Fig. 6. Variation of concentration profiles with various parameters.

imation succeeds in giving a convergent solution with increased radius of convergence. The presented model is a prototype to understand the complicated applications to practical problems such as film cooling, polymer fiber coating, coating of cylindrical wires and extrusion problems wherein nanoliquid can act as a good cooling liquid that determines the properties of the extrudate.

ACKNOWLEDGMENTS

Research is supported by the Department of Science and Technology (Government of India), New Delhi, India under the project SR/S4/MS: 409/06. The project is being implemented at the Centre for Mathematical Sciences, Banasthali University, Rajasthan, India.

REFERENCES

Abel, M. S., P. G. Siddheshwar, and N. Mahesha (2011). Numerical solution of the momentum and heat transfer equations for a hydromagnetic flow due to a stretching sheet of a non-uniform property micropolar liquid. *Appl. Math. Comput. 217*(12), 5895–5909.

Abo-Eldahab, E. M. and A. F. Ghonaim (2003). Convective heat transfer in an electrically conducting micropolar fluid at a stretching surface with uniform free stream. *App. Math. Comp. 137*, 323–336.

Akyildiz, F. T., H. Bellout, K. Vajravelu, and

R. A. VanGorder (2011). Existence results for third order nonlinear boundary value problems arising in nano boundary layer fluid flows over stretching surfaces. *Nonlinear Anal. RWA 12*(6), 2919–2930.

Anwar, M. I., I. Khan, S. Sharidan, and M. Z. Salleh (2012). Conjugate effects of heat and mass transfer of nanofluids over a nonlinear stretching sheet. *Int. J. Phys. Sci. 7*(26), 4081–4092.

Bachok, N. and A. Ishak (2009). Mixed convection boundary layer flow over a permeable vertical cylinder with prescribed surface heat flux. *Europ. J. Sci. Res. 34*(1), 46–54.

Bachok, N. and A. Ishak (2010). Flow and heat transfer over a stretching cylinder with prescribed surface heat flux. *Malaysian J. Math. Sci. 4*(2), 159–169.

Baker, G. A. (1975). *Essentials of Padé Approximants*. London: Academic Press.

Bidin, B. and N. Nazar (2009). Numerical solution of the boundary layer flow over an exponentially stretching sheet with thermal radiation. *Europ. J. Sci. Res. 33*(4), 710–717.

Buongiorno, J. (2006). Convective transport in nanofluids. *J. Heat Transfer 128*, 240–250.

Choi, S. U. S. and J. Eastman (1995). Enhancing thermal conductivity of fluids with nanoparticles. In *Proceedings of the 1995 ASME International Mechanical Engineering Congress and Exposition*, Volume FED 231/MD 66, San Francisco, USA, pp. 99–105. ASME.

Crane, L. J. (1970). Flow past a stretching plate. *J. Appl. Math. Phys. (ZAMP) 21*, 645–647.

Crane, L. J. (1975). Boundary layer flow due to a stretching cylinder. *J. Appl. Math. Phys. (ZAMP)*.

Devi, S. P. A. and J. Andrews (2011). Laminar boundary layer flow nanofluid over a flat plate. *Int. J. Appl. Math. Mech. 7*(6), 52–71.

Domb, C. and M. F. Sykes (1957). On the susceptibility of a ferromagnetic above the Curie point. In *Proceedings of the Royal Society of London. Series A, Mathematical and Physical Sciences*, Volume 240, London, pp. 214–228. The Royal Society.

Elbashbeshy, E. M. A. (2001). Heat transfer over an exponentially stretching continuous surface with suction. *Arch. Mech. 53*(6), 643–651.

Gashemi, B. and S. M. Aminossadati (2009). Natural convection heat transfer in an inclined enclosure filled with a water-*CuO* nanofluid. *Numer. Heat Transfer Part A 55*, 807–823.

Gireesha, B. J., S. Manjunatha, and C. S. Bagewadi (2014). Effect of radiation on boundary layer flow and heat transfer over a stretching sheet in the presence of free stream velocity. *J. Appl. Fluid Mech. 7*(1), 15–24.

Gupta, A. S. and T. R. Mahapatra (2003). Stagnation point flow towards a stretching surface. *The Canadian J. Chem. Eng. 81*, 258–263.

Hamad, M. A. A. (2011). Analytical solution of natural convection flow of a nanofluid over a linearly stretching sheet in the presence of magnetic field. *Int. Comm. Heat. Mass. Transfer 38*(4), 487–492.

Hamad, M. A. A., I. Pop, and M. A. I. Ismail (2011). Magnetic field effects on free convection flow of a nanofluid past a vertical semi-infinite flat plate. *Nonlinear Anal. RWA 12*(3), 1338–1346.

Hassani, M., M. M. Tabar, H. Nematia, G. Domairrya, and F. Noori (2011). An analytical solution for boundary layer flow of a nanofluid past a stretching sheet. *Int. J. Therm. Sci. 50*(11), 2256–2263.

Ishak, A. and R. Nazar (2009). Laminar boundary layer flow along a stretching cylinder. *Europ. J. Sci. Res. 36*, 22–29.

Ishak, A., R. Nazar, and I. Pop (2008). Uniform suction/blowing effect on flow and heat transfer due to a stretching cylinder. *Appl. Math. Model. 2*, 2059–2060.

Khan, S. K. and E. Sanjayanand (2005). Viscoelastic boundary layer flow and heat transfer over an exponential stretching sheet. *Int. J. Heat Mass Transfer 48*, 534–542.

Khan, W. A. and I. Pop (2010). Boundary-layer flow of a nanofluid past a stretching sheet. *Int. J. Heat Mass Transfer 53*, 2477–2483.

Kousar, N. and S. Liao (2011). Unsteady nonsimilarity boundary-layer flows caused by an impulsively stretching flat sheet. *Nonlinear Anal. RWA 12*(1), 333–342.

Lin, H. T. and Y. P. Shih (1980). Laminar boundary layer heat transfer along static and moving cylinders. *J. the Chinese Institute of Engineers 3*, 73–79.

Magyari, E. and B. Keller (1999). Heat and mass transfer in the boundary layers on an exponentially stretching continuous surface. *J. Phys. D: Appl. Phys. 32*, 577–585.

Makinde, O. D. and A. Aziz (2011). Boundary layer flow of a nanofluid past a stretching sheet with a convective boundary condition. *Int. J. Therm. Sci. 50*, 1326–1332.

Mercer, G. N. and A. J. Roberts (1990). A centre manifold description of contaminant dispersion in channels with varying flow properties. *SIAM J. Appl. Math. 50*(6), 1547–1565.

Noghrehabadi, A., M. Ghalambaz, and M. Ghalambaz (2011). A theoretical investigation of SiO_2-water nanofluid heat transfer enhancement over an isothermal stretching sheet. *Int. J. Multidisciplinary. Sci. Eng. 2*(9), 18–21.

Noghrehabadi, A., R. Pourraja, and M. Ghalambaz (2012). Effect of partial slip boundary condition on the flow and heat transfer of nanofluids past stretching sheet prescribed constant wall temperature. *Int. J. Therm. Sci. 54*, 253–261.

Nourazar, S. S., M. H. Matin, and M. Simiari (2011). The HPM applied to MHD nanofluid flow over a horizontal stretching plate. *J. Appl. Math.*, 1–17.

Partha, M. K., P. Murthy, and G. P. Rajashekhar (2005). Effect of viscous dissipation on the mixed convection heat transfer from an exponentially stretching surface. *Heat Mass Transfer 41*, 360–366.

Rana, P. and R. Bhargava (2012). Flow and heat transfer of a nanofluid over a nonlinearly stretching sheet: A numerical study. *Comm. Nonlinear Sci. Numer. Simulat. 17*(1), 212–226.

Rangi, R. R. and N. Ahmed (2012). Boundary layer flow past a stretching cylinder and heat transfer with variable thermal conductivity. *Appl. Math. 3*, 205–209.

Rosmila, A. B., R. Kandasamy, and I. Muhaimin (2012). Lie symmetry group transformation for MHD natural convection flow of nanofluid over linearly porous stretching sheet in presence of thermal stratification. *Appl. Math. Mech. 33*(5), 593–604.

Sajid, M. and T. Hayat (2008). Influence of thermal radiation on the boundary layer flow due to an exponentially stretching sheet. *Int. Commu. Heat Mass Transfer 35*, 347–356.

Sakiadis, B. C. (1961a). Boundary layer behavior on continuous solid surfaces: I. boundary layer equations for two dimensional and axisymmetric flows. *AIChE J. 7*, 26–28.

Sakiadis, B. C. (1961b). Boundary layer behavior on continuous solid surfaces: II. boundary layer on a continuous flat surface. *AIChE J. 7*, 221–225.

Sanjayanand, E. and S. K. Khan (2006). On the heat and mass transfer in a viscoelastic boundary layer flow over an exponentially stretching sheet. *Int. J. Therm. Sci. 45*, 819–828.

Sharma, P. R. and G. Singh (2009). Effects of variable thermal conductivity and heat source/sink on MHD flow near a stagnation point on a linearly stretching sheet. *J. Appl. Fluid Mech. 2*, 13–21.

Sheikhzadeh, G. A., A. Arefmanesh, and M. Mahmoodi (2011). Numerical study of natural convection in a differentially-heated rectangular cavity filled with TiO_2-water nanofluid. *J. Nano Res. 13*, 75–80.

Siddheshwar, P. G., G. N. Sekhar, and A. S. Chethan (2014a). Flow and heat transfer in a Newtonian liquid with temperature dependent properties over an exponential stretching sheet. *J. Appl. Fluid Mech. 7*(2), 367–374.

Siddheshwar, P. G., G. N. Sekhar, and A. S. Chethan (2014b). MHD flow and heat transfer of an exponential stretching sheet in a Boussinesq-Stokes suspension. *J. Appl. Fluid Mech. 7*(1), 169–176.

Singh, P., D. Sinha, and N. S. Tomer (2012). Oblique stagnation-point Darcy flow towards a stretching sheet. *J. Appl. Fluid Mech. 5*(3), 29–37.

Sinha, D., P. Jain, and N. S. Tomer (2014). Computer-assisted power series solution for MHD boundary layer flow of a weakly electrically conducting nanoliquid past a stretching sheet. *Open J. Heat Mass Momentum Transfer 2*(2), 47–57.

Vajravelu, K. and A. Hadjinicolaou (1997). Convective heat transfer in an electrically conducting fluid at a stretching surface with uniform free stream. *Int. J. Eng. Sci. 35*, 1237–1244.

Vajravelu, K., K. V. Prasad, J. Lee, C. Lee, I. Pop, and R. A. VanGorder (2011). Convective heat transfer in the flow of viscous *Ag*-water and *Cu*-water nanofluids over a stretching surface. *Int. J. Therm. Sci. 50*(5), 843–851.

Vajravelu, K., K. V. Prasad, and C.-O. Ng (2013). Unsteady convective boundary layer flow of a viscous fluid at a vertical surface with variable fluid properties. *Nonlinear Anal. RWA 14*(1), 455–464.

VanDyke, M. (1974). Analysis and improvement of perturbation series. *Mathematics & Physical Sciences 27*(4), 423–456.

VanGorder, R. A., E. Sweet, and K. Vajravelu (2010). Nano boundary layers over stretching surfaces. *Comm. Nonlinear Sci. Numer. Simulat. 15*(6), 1494–1500.

Wang, C. Y. (1988). Fluid flow due to a stretching cylinder. *Phys. Fluids 31*, 466–468.

Wang, C. Y. (2002). Flow due to a stretching boundary with partial slip-an exact solution of the Navier-Stokes equations. *Chem. Eng. Sci. 57*, 3745–3747.

Wang, C. Y. (2007). Stagnation flow on a cylinder with partial slip-an exact solution of the Navier-Stokes equations. *IMA J. Appl. Math. 72*, 271–277.

Wang, C. Y. (2009). Analysis of viscous flow due to stretching sheet with surface slip and suction. *Nonlinear Anal. RWA 10*, 375–80.

Wang, C. Y. (2012). Natural convection on a vertical stretching cylinder. *Commun. Nonlinear Sci. Numer. Simulat. 17*, 1098–1103.

Wang, C. Y. and C.-O. Ng (2011). Slip flow due a stretching cylinder. *Int. J. Nonlinear Mech. 46*, 1191–1194.

Xu, H. (2005). An explicit analytic solution for convective heat transfer in an electrically conducting fluid at a stretching surface with uniform free stream. *Int. J. Eng. Sci. 43*, 859–874.

Yacob, N. A., A. Ishak, I. Pop, and K. Vajravelu (2011). Boundary layer flow past a stretching/shrinking surface beneath an external uniform shear flow with a convective surface boundary condition in a nanofluid. *Nanoscale Res. Lett. 6*(1), 314–320.

Zhou, J. K. (1986). *Differential transformation and its applications for electrical circuits (in Chinese)*. Wuhan, China.: Huazhong University Press.